UDC 699 . 14 . 018 . 44 : 539 . 4 . 015 . 1

Alloy Design of Nano-sized Precipitates Bearing High-strength Ferritic Heat-resistant Steels

Yasushi HASEGAWA*1
Suguru YOSHIDA*1
Yutaka OKAYAMA*3
Susumu UMEKI*3
Taro MURAKI*1
Masahiro OHGAMI*2
Fumihiro KAWAZOE*3

Abstract

Precipitation site, morphology and high temperature stability of the fine carbo-nitride particles were precisely analyzed for the high strength ferritic heat resistant steels, both the 9%Cr-W containing ASME Gr. 92 and the 2.25%Cr-1%Mo-V ASME Gr. 22V. TEM observation, EDX analyses identified the fine (Nb,V) (C, N) precipitation inside of the lath structure of Gr. 92 steel and dense precipitation on the lath boundary of Gr. 22V steel. Thermodynamic calculation and the void strengthening estimation inferred that the nano-scale size particles inside of the lath structure effectively delayed the sub-grain microstructure degradation in Gr. 92 steel, and that the nano-scale size VC on the lath boundary possibly determined the creep rupture strength of Gr. 22V steel.

1. Introduction

Technical advances such as energy efficiency improvements in power plants through operation at higher temperatures and pressures and the enhancement of desulfurization efficiency of petrochemical plants through operation at higher temperatures are essential for conserving the global environment by reducing the emission of hazardous materials and CO_2. The creep strength of steel material is one of the decisive factors that determine the efficiency of facilities such as fossil power plants and distillation, refining and reduction equipment of crude oil. Improving the creep strength of ferritic heat-resistant steels used for these plant facilities is important in their design. However, with a ferritic heat-resistant steel the phase transformation temperature of which is 800 to 1,000°C, the mobility of dislocations composing the microstructure increases as the service temperature of a plant facility exceeds 500°C and approaches the transformation temperature, and the strength of the material decreases significantly as a result of the recovery of the dislocation structure.

For this reason, the alloy design of a ferritic heat-resistant steel for high-temperature applications should focus on stabilizing the dislocation structures that compose the microstructure and making the structures last at high temperatures for as long a time as possible, or suppressing the mobility of dislocations at high temperatures[1]. However, at the time of the development of ferritic heat-resistant steels for high-temperature use, the operating pressure of the subject equipment was lower than it is today, and Cr-Mo steels were used for the applications in consideration of corrosion resistance. As a result, the creep properties of the steels at high temperatures were not good enough. Higher operating temperature and pressure of the latest plants require a higher level of creep strength, and various high-creep-strength steels have been developed and applied to plant facilities.

The authors analyzed the precipitation behavior and morphology of nano-sized precipitates that bring about high-temperature creep strength (mainly (Nb,V)(C, N)) by transmission electron microscope

*1 Steel Research Laboratories
*2 Yawata R&D Lab.
*3 Nagoya Works

Table 1 Representative chemical compositions of the ASME Gr.92 and the Gr. 22V ferritic heat resistant steeels

	Chemical composition (mass%)									
	C	Si	Mn	Cr	Mo	W	V	Nb	N	B
Gr. 92	0.10	0.25	0.50	9.00	0.50	1.80	0.20	0.060	0.050	0.002
Gr. 22V	0.14	0.03	0.40	2.25	1.00		0.25			

(TEM) observation and characterization of precipitates. The specimen steels used were ASME Gr. 92 (9%Cr-1.8%W-MoNbVNB)[2], a high-Cr ferritic heat-resistant steel developed by Nippon Steel Corporation and having a tempered-martensitic structure as the parent microstructure, and ASME Gr. 22V (2.25%Cr-1%Mo-0.25%V), a standardized steel, consisting mainly of a bainitic structure and exhibiting a high creep rupture strength for low-Cr steel. **Table 1** shows the typical chemical compositions of the specimen steels. The authors also studied the creep deformation delaying effects and high-temperature stability of the precipitates and the improvement mechanisms of the high-temperature creep strength of the specimen steels. This paper reports the results of the analyses and studies.

2. Fine Precipitates in Ferritic Heat-resistant Steels

2.1 Fine precipitates inside lath structures of Gr. 92 Steel

Fig. 1 shows the creep rupture strength-time curves of ASME Gr. 92. The creep rupture strength exceeding 125 MPa at 600°C after 100,000 h is the highest of ferritic heat-resistant steels commercially used. For the creep strength to show, it is necessary to form a microstructure having a high dislocation density (tempered martensite, in this case), and at the same time, introduce factors that delay the recovery of the dislocation structure at high temperatures. The improvement of long-term creep strength is considered to depend, in particular, on how long the factors to delay the structural recovery are retained stably. The factors in the inhibition of the structural recovery of Gr. 92 so far proposed include the following: the solute dragging effects by Mo and W[2]; the dislocation gliding inhibiting effects by (Nb,V)(C, N) precipitating in fine particles inside lath structures (hereinafter referred to as the precipitation hardening by MX)[3]; and the inhibition of dynamic recrystallization by $Cr_{23}C_6$ and/or Fe_2W covering high-angle grain boundaries[4].

Many research reports have been presented over the last few years on high-temperature steels containing W, and as a consequence, the above proposed factors have been widely accepted as effective, directly or indirectly, in enhancing the high-temperature stability of tempered martensite for a long period. What is considered to be most effective of the above factors in retaining the high-temperature strength for a long period is the precipitation hardening by MX inside lath structures. **Photos 1** and **2** show TEM micrographs of the MX precipitates inside lath structures in specimens prepared by the carbon extraction replica method. The shape of the MX precipitates is classified roughly into two: Photo 1 shows granular or tabular precipitates and Photo 2 a composite precipitate called V-Wing. The latter is seldom observed before creep; VN is known to precipitate at two opposite faces of a cube-shaped NbC and grows coherently to the matrix as creep deformation advances[5].

The results of energy dispersive X-ray analysis (EDX) attached to Photo 2 show that the core of the precipitate consists mainly of Nb, and the wings mainly of V. MX precipitates were found in great

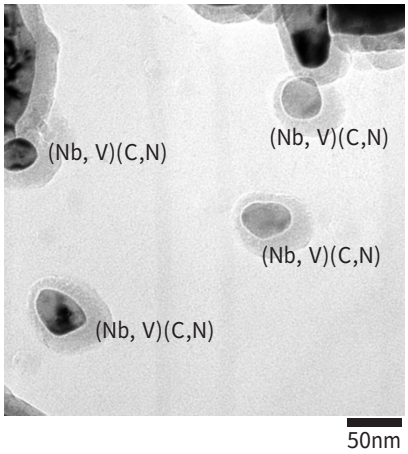

Photo 1 Granular MX observed in lath structure of Gr. 92 steel

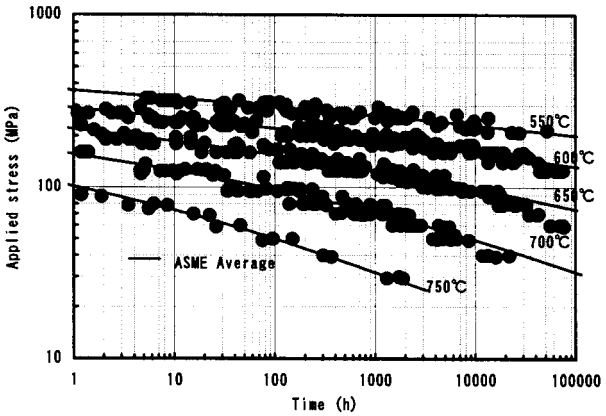

Fig. 1 Creep rupture curves of the ASME Gr. 92 steel for high temperature

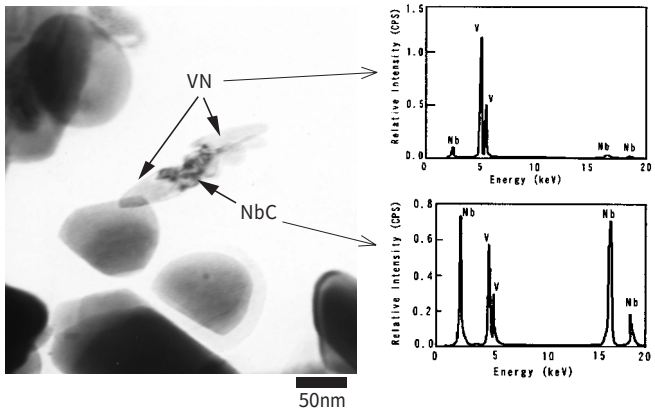

Photo 2 Morphology of NbC-VN combined type MX, V-Wing, and their EDX analyses

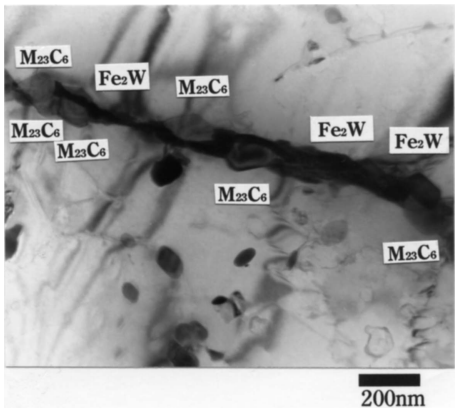

Photo 3 A congested precipitation of $M_{23}C_6$ and Fe_2W at the grain boundary of Gr. 92 steel

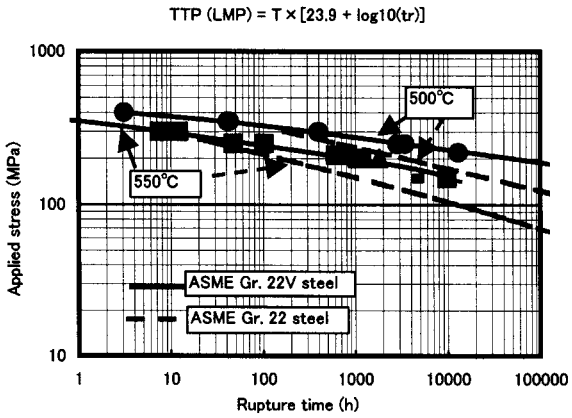

Fig. 2 Creep rupture curves of the Gr. 22V steel in comparison with those for the Gr. 22 steel

numbers inside the lath structures of Gr. 92 after a creep test at 600°C for approximately 80,000 h. The average particle size of the MX precipitates as measured with an energy-filtered TEM (EF-TEM, a high-resolution TEM having the function of producing an element distribution profile image by energy-loss spectroscopy) is, reportedly, 20 to 50 nm[6]. $(Cr, Fe)_{23}C_6$ type carbides (hereinafter referred to simply as $M_{23}C_6$) 100 to 200 nm in size were also found inside lath structures, but their precipitation density was so low compared with the MX precipitates that their contribution to intra-granular precipitation hardening was judged to be small.

It has to be noted that $M_{23}C_6$, intermetallic compounds, $(Fe, Mo)_2W$ type Laves phases, etc. precipitate on high-angle grain boundaries of Gr. 92 in particles as coarse as more than 100 nm in average size. The authors proposed a mechanism whereby these coarse grain boundary precipitates cover the boundaries as shown in **Photo 3** for a long period, delaying the deformation of block grains and packet grains, which are presumed to constitute deformation structure units, and thus indirectly stabilize the lath structures inside crystal grains [4]. Systematic quantification of the strengthening effect of these coarse precipitates is, however, a future subject.

2.2 Fine precipitates on lath boundaries in Gr. 22V steel

Fig. 2 compares creep rupture strength-rupture time curves of a steel equivalent to Gr. 22V (solid lines marked as ASME Gr. 22V steel in the graph) prepared in laboratory with those of a 2.25Cr-1Mo steel not containing V (dotted lines marked as ASME Gr. 22 steel). The representative curves were obtained by fitting the test results with cubic curves of temperature T (°C) and rupture time tr (h) using the Larson-Miller parameter (TTP (LMP) given at the top of the graph). It is clear from the graph that Gr. 22V containing 0.25% V has a creep rupture strength higher than that of Gr. 22 not containing V at both 500 and 550°C, indicating that the addition of V increases creep rupture strength. Viewing the creep test at 550°C as an accelerated test for 500°C and judging from the fact that there is no significant bend in the creep rupture curves for 550°C up to 10,000 h, one can presume that the creep rupture strength of Gr. 22V at 500°C is stable up to 100,000 h.

Photo 4 shows the microstructure observed in a thin film specimen of a test piece of Gr. 22V having crept under a constant load of 150 MPa at 550°C for 10,000 h. Fine particles of VC are found to precipitate in rows at positions indicated by arrows. Judging from the structure around the VC precipitates and the interval between the rows, the VC is presumed to have precipitated on the lath boundaries

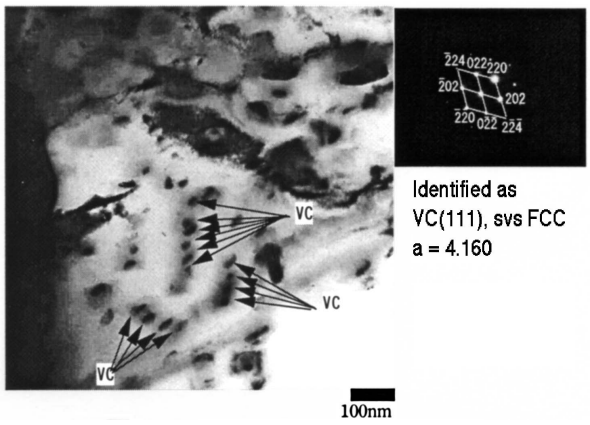

Photo 4 VC precipitation on the lath boundary of Gr. 22V steel

of tempered bainite. The VC precipitate formed because Gr. 22V contained V; the authors have confirmed its precipitation at the as-heat-treated stage before the creep test through TEM observation. The design service temperature of Gr. 22V is 450 to 500°C, lower than that of Gr. 92. Therefore, even if the VC precipitates coarsen at a rate determined by the diffusion rate of V in the steel at the lath boundaries, as far as the condition of use is limited to 500°C and up to 100,000 h, the extent of the agglomeration and coarsening of the precipitates is presumed to be more or less the same, at the most, as that in the structural observation results after the creep test at 550°C for 10,000 h.

VC and $M_{23}C_6$ were found to precipitate inside lath structures as well. However, as is clear from Photo 4, the precipitation density was higher at lath boundaries, and the effect of their precipitation to inhibit dislocation motion is presumed to be larger at the boundaries than inside the lath structures. Although some think that the precipitates inside lath structures exert greater precipitation hardening effects than those at lath boundaries do because of their high coherency with the matrix, judging from the fact that observation of the precipitates inside lath structures have disclosed that they change gradually from initial cubic shape to granular shape, it is more reasonable to think that the coherency strain has already been lost at the time Photo 4 was taken.

$(Mo, V)_2C$ and $M_{23}C_6$ were also found to precipitate on high-

angle grain boundaries, but their particles were as coarse as 100 nm or more, and precipitation in so high a density as to realize the grain boundary covering effect as seen with Gr. 92 was not observed. This means that the precipitates on high-angle grain boundaries of Gr. 22V cannot exert as large a strengthening effect as that in Gr. 92. For this reason, the observation results pointed to the possibility that the VC was the principal factor to inhibit the motion of dislocations, namely to delay the recovery of microstructure, at high temperatures.

3. Estimation of Long-term Effect of Nano-sized Precipitates to Retard Recovery of Sub-grain Structure

3.1 Estimation of strengthening by MX precipitating inside lath structures

Table 2 shows the results of measurement of the mean particle diameter of the MX precipitate inside lath structures of Gr. 92 obtained through image analysis of TEM micrographs and the results of theoretical calculation, based on the above measurement results, of the linear tension on mobile dislocations when the precipitate particles interact with them on slip planes.

At room temperature, precipitates exert repulsive force on dislocations because of the lattice strain resulting from the coherence between the precipitates and the matrix, and as a consequence, the Orowan stress arises, which is the linear tension that is caused when a dislocation passes through an inter-particle space. At high temperatures, on the other hand, the coherence between the precipitates and the matrix is lost within a short period as a result of the coherence relaxation by dislocations, and therefore the repulsive force scarcely forms. However, the interface of a particle has the same effect as a void does, and thus a dislocation line is trapped into an interface owing to an absorption effect, and the amount of energy required for escaping from there is expended[7]. Slorovitz et al.[8] proposed the following theoretical equation to calculate the linear tension that is exerted when a dislocation line that was trapped between incoherent particles bows out from there:

$$\sigma_{sl} = A_\nu \frac{MbE}{4\pi(1+\nu)\lambda}\left[1n\left(\frac{L}{r_0}\right) + 0.7\right] \qquad A_\nu = \left(1 - \frac{\nu}{1-\nu}\sin^2\varphi\right)\cos\varphi \tag{1}$$

where M is Taylor's factor (2.5), b is the Burgers vector length (0.248 nm), E is the Young's modulus at service temperature (170 GPa), L is the harmonic mean distance between precipitate particles, r_0 is the cut-off radius of a dislocation core (estimated at approximately $5b$), λ is the measured mean distance between particle surfaces, ν is Poisson's ratio (0.31), and φ is the angle of escape of a dislocation from an inter-particle space between incoherent precipitates, which is 0.19 (rad) assuming that all dislocations that interact with the particles are edge dislocations.

The precipitation strengthening stress in Table 2 was calculated using Equation (1) on a simple assumption that all the precipitate particles are spherical and they are distributed squarely, that is, evenly at points of a space lattice. Precipitate particles may be viewed as spherical in some cases, but in reality, particles having the same volume may have various shapes that allow wide interactions with dislocations, such as the V-Wing. However, the rate of the formation of V-Wings is not very high: it was less than 10% in the extraction replicas. Table 2 also shows the calculation results of the void strengthening stress on an assumption that the V-Wings account for approximately 10% of all the MX precipitates (the column of "MX with V-Wing"). The values include measurement errors of ±7 to 10 MPa. The precipitation of the V-Wings increases the strengthening stress slightly.

MX does not precipitate evenly inside lath structures in reality. However, the gliding of dislocations determines the rate of material deformation in the temperature range where ferritic heat-resistant steels, which have a martensitic structure strengthened by the precipitation of fine carbonitrides, such as Gr. 92 deform as a result of the dragging motion of dislocations[9]. For this reason, the inhomogeneity of microstructure and precipitate does not pose any significant problem in the calculation, and it is possible to assume that the mean distance between such inhibiting agents determines deformation resistance. This does not mean that the calculation results in Table 2 are unrealistic, but rather, the calculation results on the said assumption of the presence ratio of V-Wings may be overestimating the strengthening stress, because the assumed presence ratio was larger than it really is.

Summing up the discussions above, the calculation results in Table 2 predict that the strengthening stress by the precipitation of MX in Gr. 92 is not so large as to be comparable to creep rupture strength. Therefore, thinking that the MX type precipitates inside lath structures are responsible for the material strengthening of the Gr. 92 steel purely through a secondary effect of inhibiting the decrease in dislocation density explains the calculation results most suitably.

3.2 Estimation of strengthening by VC precipitating on lath boundaries

Table 3 compares calculations of two kinds of strengthening stress in Gr. 22V. One is the strengthening stress resulting from the precipitates inside lath structures on an assumption that Equation (1) applies, and the other is the strengthening stress resulting from the inhibition of the move of lath boundaries (more specifically the degradation of lath structures into sub-grains), on an assumption that VC that precipitates on a lath boundary inhibits the dislocations that compose the lath boundary from escaping from their positions, or prevents the change of lath structures into equiaxed grains. Note that 0.35 was used here as the value of ν in Equation (1) considering that it was close to that in a 2.25Cr-1Mo steel. The calculation results in Table 3, although they include measurement errors of ±50 MPa, indicate that the precipitation of VC in rows on lath boundaries seen with Gr. 22V creates large precipitation strengthening stress comparable to the creep rupture strength of the steel. This means that, when VC precipitates on lath boundaries in a high density in-

Table 2 Estimated precipitation strengthening stress in lath structure of Gr. 92 steel

	Spherical MX	MX with V-Wing
Mean particle diameter	50nm	120nm
Inter partcle space	630nm	600nm
σ_{sl} at 650°C for 10,000 hours creep	35MPa	50MPa

Table 3 Estimated precipitation strengthening stress in lath structure of Gr. 22V steel

	Lath interior	Lath boundary
Mean particle diameter	50nm	20nm
Inter partcle space	353nm	48nm
σ_{sl} at 550°C for 10,000 hours creep	41MPa	205MPa

hibiting the coarsening of lath structures together with a low service temperature, the lath boundary fixing by the precipitates alone can explain the high creep rupture strength retained for a long period. Note that it is necessary in this case to set forth an assumption that the movement velocity of a dislocation is determined almost by the time of its escape from a lath boundary, and thus a dislocation is supposed to move virtually freely inside a lath structure. The reason for this is that the lath structures of Gr. 22V are, different from the same of Gr. 92, those introduced through bainite transformation, and the density of dislocations inside them are not very high and the lath width is large.

The estimation results point to the possibility of material strengthening by making the strengthening factors concentrate at portions where internal stress is high (in the case of the present paper, at lath boundaries, where dislocation density is high). Note that, from the facts that there are various kinds of dislocations at a high-angle grain boundary, and that interface energy is low and elements having large atomic radii can easily diffuse there, the authors assumed that precipitates were likely to coarsen at such grain boundaries as described earlier, and the coarse precipitates did not contribute to the strengthening of the material significantly unless they cover the grain boundary completely to freeze the dislocation structure inside the grains.

4. High-temperature Stability of Nano-sized Precipitates

The authors explained in the preceding sections that the fine carbonitrides were important as a strengthening factor also at high temperatures. For maintaining high creep rupture strength, it is necessary for precipitation strengthening particles to last for a long period and suffer only a little change over time. Through heat treatment, Nb and V, the main component elements of the MX particles, precipitate as carbonitrides nearly in the equilibrium amounts at the service temperature of plant facilities. If these precipitates are in a phase that is stable under the service condition, they undergo Ostwald ripening with the lapse of time and agglomerate into coarse particles. This means that the change of material properties that occurs is only the change determined by the rate of diffusion, and it is possible to estimate the material properties after the lapse of a certain time phenomenologically and qualitatively.

Fig. 3 shows the results of the estimation of the equilibrium phases at 600°C of precipitates in ferritic steels containing Cr by 1 to 10% using Thermo-Calc[10, 11]. The database used was SSOL2. Only those precipitate phases that were identified by TEM observation and the quantitative chemical analysis and qualitative X-ray diffraction analysis of the extraction residue obtained by controlled potential electrolysis were assumed to be stable in the estimation. Among the component elements of the MX precipitates, the content of V is plotted along the ordinate of the diagram and that of Cr along the abscissa. The black star in the diagram indicates the chemistry of Gr. 92. The MX type precipitates are extremely stable in all the graph regions, and M_2X cannot exist in the region where the V content is 0.15% or more. The calculation results shown in the graph agree well with observation results.

A paper reported that a Z phase, or (Cr, Nb)VN, precipitated near high-angle grain boundaries of Gr. 92 and MX decreased there during a creep test for more than 50,000 h at 650°C[12], but the authors failed to confirm it through creep rupture tests of the steel at 600°C for up to 100,000 h. Using a TEM, the authors also observed real Gr. 92 boiler tubes that had been used at 560 to 590°C for 50,000 to 110,000 h as the superheater tubes of a commercially operated plant and dismounted from it, and any change in precipitate phase was not observed either.

Fig. 4 is an estimated phase diagram at 500°C of steel containing 1% Mo; the authors used it for the study of the MX precipitates in the equilibrium phase of Gr. 22V. The white star in the diagram indicates the chemistry of Gr. 22V. The graph shows that the MX precipitates can exist in Gr. 22V stably in wide regions, as they can in Gr. 92. VC was found through the analysis of precipitate phases by TEM observation and the X-ray diffraction spectroscopy of the extraction residue after an accelerated test at 550°C, but no phases other than those in the calculated phase diagram were found to precipitate. This seems to mean that as far as the studies up to the present are concerned, VC, which is presumed to be the principal strengthening factor, does not undergo any phase transformation at 500°C.

As a conclusion, it is reasonable to think that the rapid degradation of fine MX precipitates, the principal strengthening factor, does not occur in either Gr. 92 or Gr. 22V up to 100,000 h of use in their service temperature range. Thus, through the estimation of precipitation strengthening stress, the present study demonstrates the possibility that the nano-sized precipitates serve for a long period as obstacles to the move of dislocations, and therefore act as the secondary factor in the strengthening of Gr. 92, and as the principal factor in that of Gr. 22V.

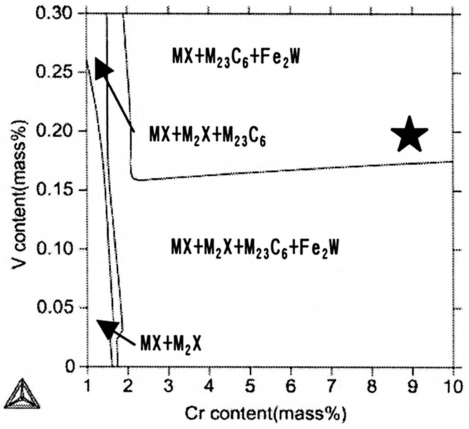

Fig. 3 Calculated phases as a function of Cr and V content at 600°C for 1%Mo containing steel

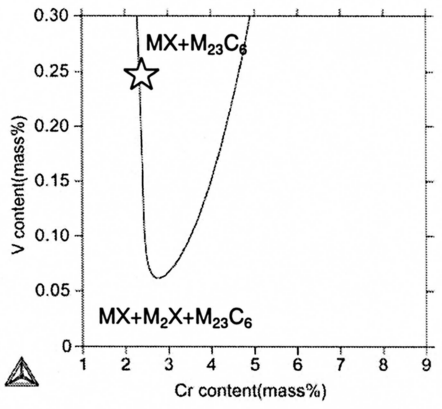

Fig. 4 Calculated phases as a function of Cr and V content at 500°C for 1%Mo containing steel

5. Summary

Nano-sized carbonitride particles that precipitate inside lath structures and on the boundaries therebetween are presumed to be the factor that retains the high creep strength of ferritic heat-resistant steels, ASME Gr. 92 and Gr. 22V, for a long period. The authors examined the morphology and high-temperature stability of the particles in detail, and estimated the precipitation strengthening stress brought about by the fine precipitates. As a conclusion, it is reasonable to think that, in Gr. 92, the precipitation of (Nb,V)(C, N) inside lath structures delays the recovery of dislocation structures, contributing to the increase in creep strength, and in Gr. 22V, the precipitation of VC on lath boundaries serves as the principal factor in increasing creep strength.

References

1) Nakajima, E. et al.: Report of the 123rd Committee on Heat-Resisting Materials and Alloys, Japan Society for the Promotion of Science. 42, 2001, p. 173
2) Ohgami, M. et al.: Shinnittetsu Giho. (362), 49(1997)
3) Nishimura, N. et al. Key Engineering Materials. 171-174, 297(2000)
4) Hasegawa, Y. et al.: J. of the Soc. of Materials Science Japan. 52(7), 843 (2003)
5) Hamada, K. et al.: Nuclear Engineering and Design. 139, 227(1993)
6) Hald, J. et al.: ISIJ International. 43(3), 420(2003)
7) Hayakawa, H. et al.: J. of the Japan Institute of Metals. 67(1), 22 (2003)
8) Srolovitz, D. J. et al.: Phil. Mag. A48, 795(1983)
9) Hayakawa, H. et al.: Tetsu-to-Hagané. 89(10), 72(2003)
10) Sundman, B. et al.: Calphad. 9, 153(1985)
11) Royal Institute of Technology: SGTE Solution Database of Jan. ed. Sundman, Sweden, 1994
12) Suzuki, K. et al.: Tetsu-to-Hagané. 86, 550(2000)